INTERNATIONAL JOURNAL OF ADVANCE RESEARCH, IDEAS AND INNOVATIONS IN TECHNOLOGY

ISSN: 2454-132X
Impact factor: 4.295
(Volume 4, Issue 4)
Available online at: www.ijariit.com

RSM application for optimization of ECMM parameter using S1 Tool steel

Love Kishore Sharma
sharma.ajmer31@gmail.com
Jaipur Institute of Technology, Jaipur, Rajasthan

Dilip Gehlot
dlpgehlot@ecaajmer.ac.in
Government Engineering College, Ajmer, Rajasthan

Anil Kumar Sharma
principaljit2017@gmail.com
Jaipur Institute of Technology, Jaipur, Rajasthan

Bhupendra Verma
bhup95in@yahoo.co.in
Government Engineering College, Ajmer, Rajasthan

ABSTRACT

S1 tool steel (60WCrV7) are used for the production of cold shear knives, ejector pins, air hammers etc. It is very difficult to machine S1 Tool steel alloys using conventional machine tools due to high toughness, impact resistance, dimensional stability and high hardening capacity. The Electrochemical Machining (ECM), a non-traditional manufacturing process, is a prime choice for machining S1 Tool steel alloys. The main aim in present work is to investigate the influence of ECM process parameters, such as applied voltage (V), the inter-electrode gap (IEG), electrolyte flow rate (F.R.) and electrolyte concentration (EC), on Radial Overcut (ROC) during machining S1 Tool steel material. An aqueous solution of sodium nitrate (NaNO3) is used as an electrolyte. The experimental strategy depends on design formulated using response surface methodology. The effects of process parameters as well as their interactions are investigated and the process parameters are optimized by application of the response surface methodology.

Keywords: *Electrochemical Micro Machining (ECMM), Radial Over Cut (ROC), S1 Tool steel*

1. INTRODUCTION

In electrochemical machining (ECM) no contact between metal and electrode exists. A mirror image of the tool is imprinted on workpiece [1]. ECM is used for difficult-to-cut materials and with complex geometry. A D.C. voltage (5-30 V) is applied across the IEG between pre-shaped cathode tool and an anode workpiece. The electrolyte flows at a high speed through the IEG the anodic dissolution rate, which is governed by Faraday's laws of electrolysis, depends on the chemical properties of work material type of electrolyte used and current supplied. The by-products generated during the machining are removed by the high-velocity flow rate of the electrolyte. In the ECM process, no thermal affected machine zone exists also a high-quality surface texture is obtained. With the increasing demands of micro products and difficult to machine materials in aerospace, automotive, electronics, optics and medical devices, the concept of ECMM is applied to its full extent. ECMM overcomes the disadvantages of other machining processes i.e. no tool wear, comparable high MRR and complex part production with no stress and cracks induced on free surfaces [2]. ECMM has been widely used for manufacturing turbine blades, engine castings, gears, dies and moulds and surgical implants. It is also implemented for mass or batch production. S1 Tool steel material is better than any other commonly used nickel-based alloys due to its high toughness and high hardening. Its alloys work hardens rapidly as it goes through high strains during machining. This hardening effect slows further machining. Therefore, it becomes extremely difficult to machine these alloys by application of conventional machine processes. ECMM is thus a cost-effective alternative for S1 Tool steel material and could become highly significant in the coming future. Numerous works have been elaborated in the literature for machining of nickel-based alloys using different non-conventional machining methods. The advancement in the machining of nickel base and titanium alloys with ceramic tools was briefly examined by Ezugwu *et al.* [3, 4]. Liu *et al.* studied the characterization of nickel alloy micro-holes using micro-EDM together with grinding [5] Ulutan *et al.* analysed machining-induced surface integrity for titanium alloys and nickel-based alloys. Problems with residual stresses, white layer and work hardening layers, as well as microstructural alterations were studied to improve surface qualities of end products [6]. Selvakumar *et al.* [7, 8] investigated the machining suitability of alloys with wire-cut electrical discharge machining (WEDM). Die corner accuracy and surface roughness were considered as responses; Selvakumar *et al.* [9, 10] also studied various WEDM process parameters' influence. Significant efforts [9-12] have been made on the machining of nickel-based alloys. The major disadvantage of these machining methods, elaborated in the literature, resulting in the deterioration of tool life including WEDM. But the machining suitability of S1 Tool steel alloys, with ECM process, is not widely reported in the literature. Hence, in the current work, ECMM is mainly studied for determining S1 tool steel

characteristics. A mathematical model interactive higher order influences of the different machining parameters such as voltage (V), inter-electrode gap (IEG), electrolyte concentration (EC) and electrolyte flow rate (F.R.) on performance parameter Radial Overcut (ROC). RSM concept is applied for planning and analyzing the design of experiments. RSM is selected for investigating the response over entire factor space along with the location of the zone where the response reaches its near optimum values. A thorough analysis of response surface models, a combination of parameters is obtained which provides the best output.

2. EXPERIMENTAL SETUP

A schematic diagram of the ECMM set-up is described in Figure 1. The natural variables opted for the present research, are EC, V, FR, and IEG. A copper electrode with a diameter of 0.16 mm is used as tool material. Other materials like Aluminium, brass, iron etc. can also be used as tool electrode. The machining time is made constant for all the experiments i.e. 30 minutes.

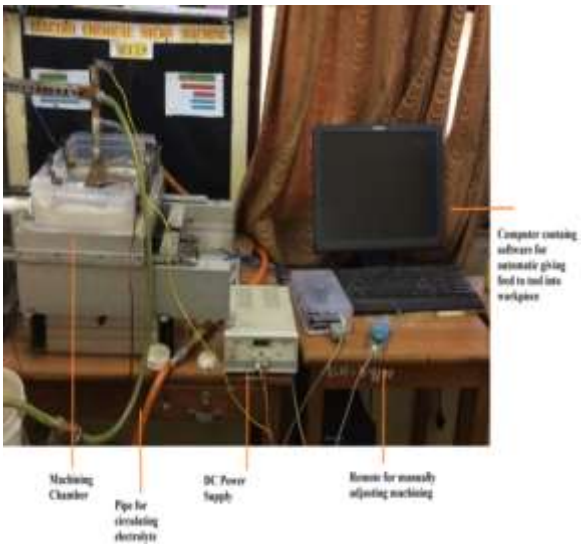

Fig. 1: ECMM Setup

Their combined effects on ROC are evaluated through the set of the experiments based on Box Behnken design (BBD) of RSM. Table.1 shows the factors and their levels in coded the levels of each factor were chosen as -1, 0, 1 in such a manner as to form a rotatable design.

Table 1: ECMM machining parameters and levels

Parameters/ Level	Low	Mid	High
Voltage(V), X1	20	25	30
E C (gm/ltr),X2	150	175	200
I.E.G(mm), X3	0.5	1.0	1.5
FR(ltr/min), X4	2.18	4.09	6.0

The design generates 27 experiments for the four variables. The design was generated and analyzed using Minitab 17.0 statistical package.

The value of ROC is obtained from below equation:

$$ROC = (Di - Do) \div 2 \qquad (1)$$

Where Di is the inner diameter of the hole produced after machining, Do is the outer diameter of tool material. Using a USB digital microscope the values of hole diameter are determined as shown in Figure 2. The software used for diameter analysis is Coolingtech.

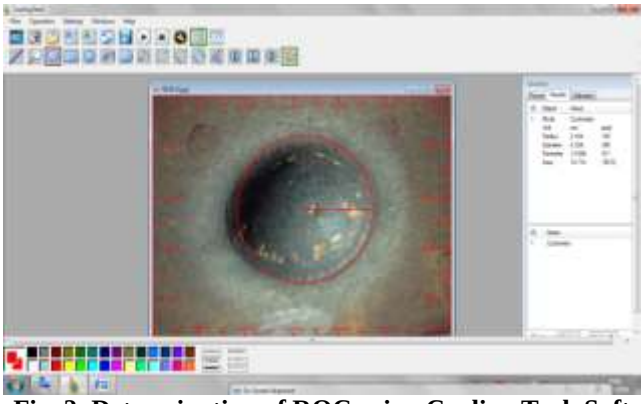

Fig. 2: **Determination of ROC using Cooling Tech Soft**

S1 Tool steel pieces with 0.2mm thickness and dimensions 1.5cm x 2.5 cm were used as a test specimen. The chemical composition (weight %) of S1 Tool steel alloys is as follows: C: 0.40-0.55, Si: 0.15-1.20, Mn: 0.10-0.40, P: MAX 0.030, S: MAX 0.030, Cr: 1.00-1.00, Mo: MAX 0.50, V:0.15- 0.30, W: 1.5-3.00.

The ROC values are obtained for a different set of experiments with a different combination of process parameters based on RSM. A second order polynomial response surface mathematical model, which explains the parametric influences on the various response criteria, is given below:

$$Y = x_0 + x_1\beta_1 + x_2\beta_2 + x_{11}\beta_1^2 + x_{22}\beta_2^2 + \ldots x_{ij}\beta_i\beta_j + \varepsilon \qquad (2)$$

In the above equation, Y is the response i.e. ROC while x_1, x_2… are the regression coefficients, **ε** represents an error that often occurs while performing experiments either due to human or environmental factors. The response table for ROC is shown below. Figure 3 shows the image of the workpiece (hole image) obtained after machining.

Table 2: Response table for machining

S. No.	*X(1)*	X(2)	*X(3)*	*X(4)*	ROC
1	0	0	1	-1	1.32055
2	1	0	0	-1	1.593166
3	0	-1	1	0	1.0155
4	-1	0	0	-1	1.528221
5	0	-1	-1	0	1.4358
6	0	1	0	1	1.49045
7	0	0	-1	1	1.570145
8	-1	0	-1	0	2.080592
9	0	0	0	0	1.319912
10	1	0	1	0	1.169049
11	0	1	-1	0	2.000677
12	0	1	0	-1	1.083812
13	0	0	0	0	1.28194
14	0	0	1	1	1.54135
15	1	0	-1	0	1.286683
16	0	-1	0	1	1.37538
17	-1	0	0	1	1.662701
18	1	0	0	1	0.785436
19	-1	-1	0	0	1.265634
20	0	0	-1	-1	1.543166
21	1	-1	0	0	1.572391
22	0	1	1	0	1.653166
23	0	0	0	0	1.48417
24	0	-1	0	-1	1.2184
25	1	1	0	0	1.694184
26	-1	1	0	0	1.17272
27	-1	0	1	0	1.488697

Fig. 3: Workpiece image after machining

3. ANOVA ANALYSIS

ANOVA test is performed to check the validity of the proposed model. The R^2 values for ROC are found to be 94.63% also value of R^2 adjusted is 88.37%. These values show that the proposed model is statistically good. Also, the P values for all the terms are studied for checking the significance of proposed terms. P values < 0.05 are significant and provide a maximum contribution to the developed model. The terms that are found to be significant are x(1), x(2), x(3), x(4), $x(1)^2$, $x(4)^2$, x(1)*x(2), x(2)*x(3), x(2)*x(4). P values greater than 0.05 are insignificant and can be discarded. Discarding the insignificant terms further increases the adequacy of the model generated.

3.1 Regression Equation for ROC

ROC=-17.19+0.564*X(1)+0.0975*X(2)+1.443*X(3) +0.744*X(4)-0.00647*X(1)*X(1)-0.000076*X(2)*X(2)-0.255*X(3)*X(3)-0.0274*X(4)*X(4)-0.001365*X(1)*X(2)-0.0100*X(1)*X(3) +0.0074 *X(1)*X(4)-0.00731*X(2)*X(3)-0.004615*X(2)*X(4) +0.0653* X(3) *X(4) (3)

The above equation represents a full quadratic mathematical model for response ROC in terms of process parameters. Using equation 3 various graphs are plotted which defines the effects of every individual parameter on the response output.

4. RESULTS AND DISCUSSION

As per the model generated through BBD sets of the experiment, the effect of various input parameters on ROC is as follows.

4.1. Parametric Influence on ROC

4.1.1Effect of Voltage on ROC

The plot between Voltage and ROC of the experiment is shown in Fig 4 On increasing the value of applied voltage the ROC increases in a non-linear manner. Low voltage results in lower intensity electric field that further reduced the stray current effect, therefore reducing the overcut. Hence at low applied voltage ROC decreases. Increasing the applied voltage while keeping other factors constant results in an increased value of electrolyzing current available in the machining gap. This increases the overcut phenomena. Hence ROC increases.

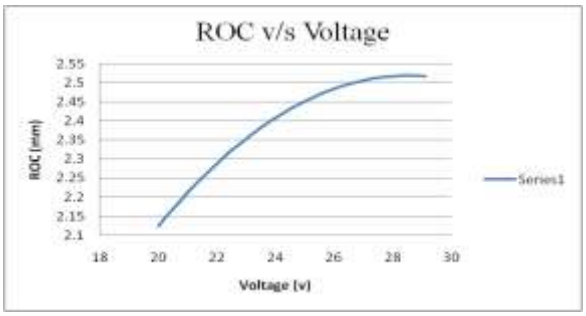

Fig. 4: ROC v/s Voltage

4.1.2 Effect of Electrolyte Concentration on ROC

The plot between Electrolyte Concentration and ROC of the experiment is shown in Fig 5 According to this fig, we can say that ROC increases with an increase in electrolyte concentration in a linear manner. This is because of increasing the metal ion concentration for a preset value of voltage, IEG and flow rate leads to the formation of a higher level of reaction products i.e. sludge and precipitates also initiate H_2, O_2 gas bubbles formation. All these effects lead to the passage of stray current in the machining zone.

Table 3: Analysis of Variance Table for ROC

Source	DF	Seq SS	Contribution	Adj SS	Adj MS	F-Value	P-Value
Model	14	1.90862	94.63%	1.90862	0.13633	15.11	0
Linear	4	1.37202	68.03%	1.37202	0.343	38.03	0
Voltage	1	0.14789	7.33%	0.14789	0.14789	16.4	0.002
Conc	1	0.84267	41.78%	0.84267	0.84267	93.42	0
IEG	1	0.32485	16.11%	0.32485	0.32485	36.01	0
Flow	1	0.0566	2.81%	0.0566	0.0566	6.28	0.028
Square	4	0.1542	7.65%	0.1542	0.03855	4.27	0.022
Voltage*Voltage	1	0.09517	4.72%	0.1394	0.1394	15.45	0.002
Conc*Conc	1	0.00027	0.01%	0.01199	0.01199	1.33	0.271
IEG*IEG	1	0.00553	0.27%	0.02161	0.02161	2.4	0.148
Flow*Flow	1	0.05323	2.64%	0.05323	0.05323	5.9	0.032
2-Way Interaction	6	0.38241	18.96%	0.38241	0.06374	7.07	0.002
Voltage*Conc	1	0.11645	5.77%	0.11645	0.11645	12.91	0.004
Voltage*IEG	1	0.0025	0.12%	0.0025	0.0025	0.28	0.608
Voltage*Flow	1	0.02021	1.00%	0.02021	0.02021	2.24	0.16
Conc*IEG	1	0.03342	1.66%	0.03342	0.03342	3.71	0.078
Conc*Flow	1	0.19427	9.63%	0.19427	0.19427	21.54	0.001
IEG*Flow	1	0.01555	0.77%	0.01555	0.01555	1.72	0.214
Error	12	0.10824	5.37%	0.10824	0.00902		
Lack-of-Fit	10	0.10218	5.07%	0.10218	0.01022	3.37	0.251
Pure Error	2	0.00607	0.30%	0.00607	0.00303		
Total	26	2.01687	100.00%				

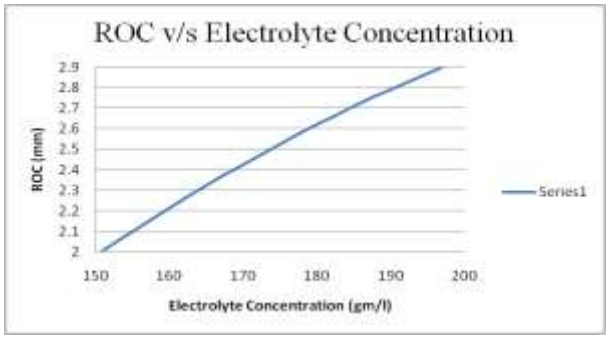

Fig. 5: ROC v/s Electrolyte Concentration

4.1.3 Effect of IEG on ROC

The plot between IEG and ROC of the experiment is shown in figure 6 According to this figure on increasing the inter-electrode gap the ROC decreases non-linearly because of increase in resistance between tool and workpiece. This leads to a decrease in the stray current density and hence the low value of ROC.

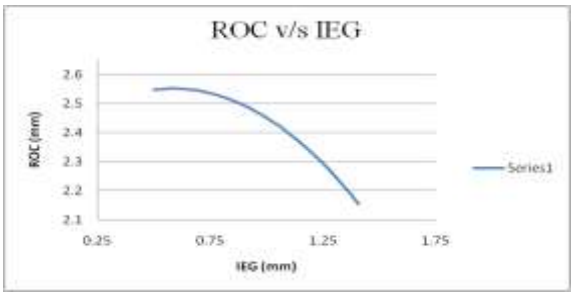

Fig. 6: ROC v/s IEG

4.1.4 Effect of Electrolyte Flow Rate on ROC

The plot between Electrolyte Flow Rate and MRR of the experiment is shown in figure 7. According to this Fig. in increasing the flow rate, the ROC increases almost linearly due to a greater volume of electrolytic ions available in the machining zone. This leads to greater stray current effect at the side wall resulting in a higher value of ROC. After optimum value, the ROC decreases due to less time available to ions for participating in reactions.

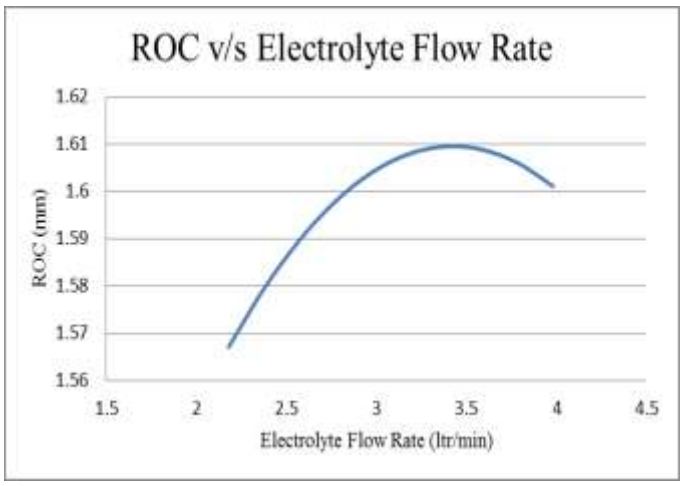

Fig. 7: ROC v/s Flow Rate

4.2 Percentage Contribution of Input Parameters on ROC

The contribution of various input parameters on ROC is shown in the Fig.8 According to this fig, we can say that contribution of electrolyte concentration is (41.78%) is maximum on ROC followed by IEG (16.11%), applied voltage (7.33%) and flow rate (2.81%).

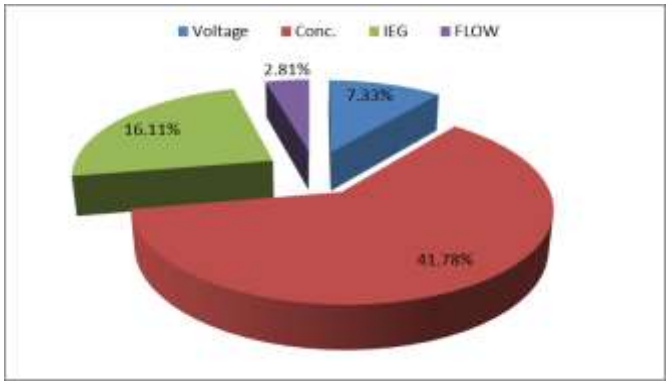

Fig. 8: Percentage contribution of input parameters on ROC

4.3 Surface Plots for Input Parameters v/s ROC

4.3.1 Effect of Electrolyte Concentration and Voltage on ROC

Figure 9 shows Surface plot between ROC and electrolyte concentration and voltage. It is clearly seen that the value of ROC increases significantly with an increase in the value of electrolyte concentration, while ROC increases slowly with applied voltage.

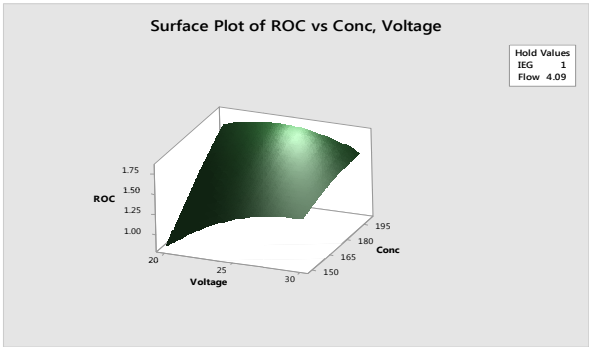

Fig. 9: ROC v/s Electrolyte Concentration, Voltage

4.3.2 Effect of Electrolyte Flow Rate and Electrolyte Concentration on ROC

Figure 10 shows Surface plot between ROC and electrolyte concentration and electrolyte flow rate. It is clearly seen that the value of ROC increases significantly with an increase in the value of electrolyte concentration, while ROC increases slowly with the electrolyte flow rate.

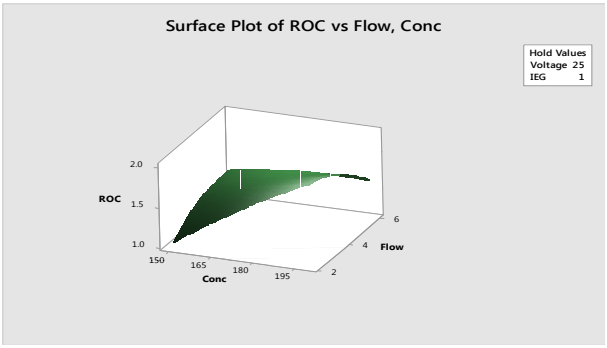

Fig. 10: Surface Plot ROC v/s Electrolyte Concentration, Electrolyte Flow Rate

4.3.3 Effect of IEG & Electrolyte Concentration on ROC

Figure 11 shows Surface plot between ROC and electrolyte concentration and IEG. It is clearly seen that the value of ROC increases significantly with an increase in the value of electrolyte concentration, while ROC decreases with increasing IEG.

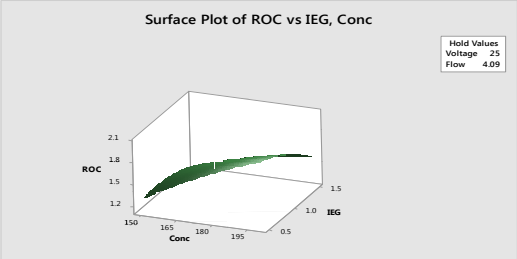

Fig. 11: Surface plot ROC v/s electrolyte concentration, IEG

4.3.4 Effect of electrolyte flow rate and voltage on ROC

Figure 12 shows Surface plot between ROC and electrolyte flow rate and voltage. It is clearly seen that for any value of voltage the ROC first increases with flow rate reaching its maximum value and then decreases.

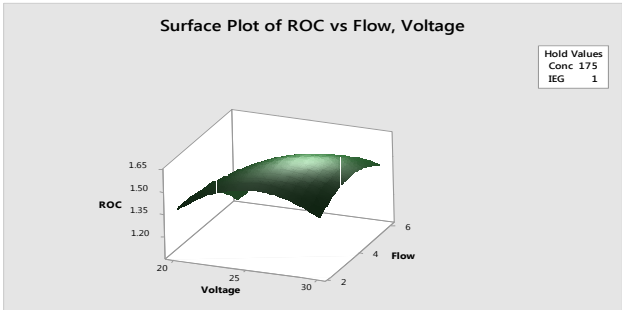

Fig. 12: Surface plot ROC v/s electrolyte flow rate, voltage

4.3.5 Effect of IEG and Voltage on ROC

Figure 13 shows Surface plot between ROC and IEG and voltage. It is clearly seen that for the low value of ROC is obtained at higher IEG and low applied voltage, while a high value of ROC is obtained at a low value of IEG and higher applied voltage.

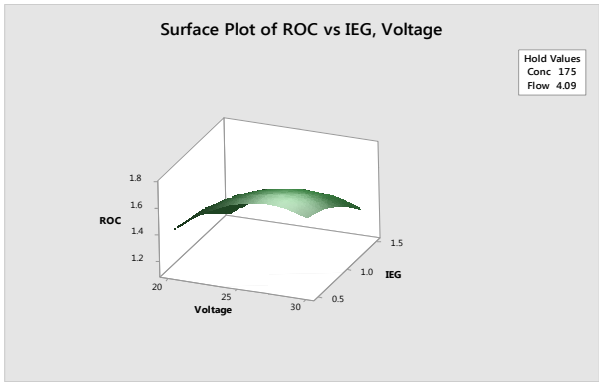

Fig. 13: Surface plot ROC v/s IEG, voltage

4.3.6 Effect of electrolyte flow rate & IEG on ROC

Figure 14 shows Surface plot between ROC and IEG and electrolyte flow rate. It is clearly seen that for the low value of ROC is obtained at higher IEG and low electrolyte flow rate, while a high value of ROC is obtained at a low value of IEG and intermediate value of electrolyte flow rate.

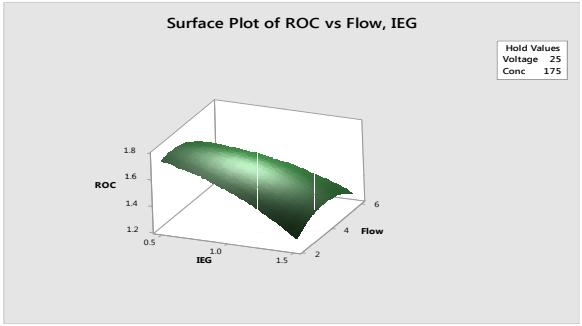

Fig. 14: Surface plot ROC v/s IEG, electrolyte flow rate

5. CONCLUSION

In the present study, four independent variables are considered namely applied voltage, electrolyte concentration, flow rate and I.E.G. S1 tool steel as a work-piece and 27 experiments are conducted to obtain an optimum level in achieving minimum Radial Over Cut (ROC). The following conclusions arrive:

1. It has been determined using Response Surface Methodology that the optimum parameters are applied a voltage of 20 V, electrolyte concentration of 150 gm/ liter, the flow rate of 2.18 liter/minute and an inter-electrode gap of 1.5 mm gives minimum ROC of 0.4861 mm.
2. ANOVA test for ROC revels that R^2 94.63% and R^2 (adj) 88.37% which confirms the significance of developed models. The p-value of terms is less than 0.05 which confirms the validity of the model used.
3. It has been found that the effect of electrolyte concentration is maximum on ROC followed by IEG, applied voltage, and electrolyte flow rate.

6. REFERENCES

[1] Rajurkar K.P, Sundaram M.M and Malshe A. P, "Review of Electrochemical and Electro Discharge Machining", Procedia CIRP, Vol. 6 (2013) 13-26, The Seventeenth CIRP Conference on Electro Physical and Chemical Machining (ISEM).

[2] Rajurkar K.P, Zhu D, McGeough J.A, Kozak J and De Silva A, "New Developments in Electro-Chemical Machining", CIRP Annals - Manufacturing Technology, Vol. 48 (1999) Issue 2, 567–579.

[3] Sundaram M.M. and Rajurkar K.P, "Electrical and Electrochemical Processes, in Intelligent Energy Field Manufacturing", CRC Press (2010) 173-212.

[4] Ezugwu E.O, "Key improvements in the machining of difficult-to-cut aerospace superalloys', International Journal of Machine Tools and Manufacture, Vol. 45(2005) Issues 12–13, 1353–1367

[5] Ezugwu E.O, Bonney J, Fadare D.A and Sales W.F, "Machining of nickel-base, Inconel 718, alloy with ceramic tools under finishing conditions with various coolant supply pressures", Journal of Materials Processing Technology, Vol. 162–163(2005) issue 15, 609–614.

[6] Liu H.S, Yan B.H, Huang F.Y and Qiu K.H, "A study on the characterization of high nickel alloy micro-holes using micro-EDM and their applications", Journal of Materials Processing Technology, Vol. 169(2005) Issue 3, 418–426.

[7] Durul Ulutan and Tugrul Ozel, "Machining induced surface integrity in titanium and nickel alloys: A review", International Journal of Machine Tools and Manufacture, Vol. 51(2011) Issue 3, 250–280.

[8] Selvakumar G, Sarkar K and Mitra S, "Experimental analysis on WEDM of S1 Tool steel alloys in a range of thickness", International Journal of Modern Manufacturing Technologies, Vol. IV (2012) 113-120.

[9] Selvakumar G, Sarkar K and Mitra S, "Experimental investigation on die corner accuracy for wire electrical discharge machining of S1 Tool steel alloy", Proc IMechE Part B: J Engineering Manufacture, Vol. 226 (2012) 10, 1694– 1704.

[10] Theisen W and Schuermann A, "Electro discharge machining of nickel-titanium shape memory alloys", Materials Science and Engineering: A, Vol. 378 (2004) Issues 1–2, 200–204.

[11] Kaynak Y, Karaca H.E, Noebe R.D and Jawahir I.S, "Tool-wear analysis in cryogenic machining of *NiTi* shape memory alloys: A comparison of tool-wear performance

with dry and MQL machining Wear", Vol. 306 (2013) Issues 1–2, 51–63.

[12] Curtis D.T, Soo S.L, Aspinwall D.K and Sage C, "Electrochemical super abrasive machining of a nickel-based aero engine alloy using mounted grinding points", CIRP Annals-Manufacturing Technology", Vol. 58 (2009) Issue 1,173–176.

[13] Gao D, Hao Z, Han R, Chang Y and Muguthu J.N, "Study of cutting deformation in machining nickel-based alloy Inconel 718", International Journal of Machine Tools and Manufacture, Vol. 51(2011) Issue 6, 520–527.

[14] Montgomary Douglas C, "Design and Analysis of Experiments" 5th edition (1997), John wiley publications, Singapore.

[15] Kadirgama K, Noor M.M, Zuki N.M, Rahman M.M, Rejab M.R.M, Daud R and Abou-El-Hossein K. A, "Optimization of Surface Roughness in End Milling on Mould Aluminium Alloys (AA6061-T6) Using Response Surface Method and Radial Basis Function Network", Jordan Journal of Mechanical and Industrial Engineering, Vol. 2 (2008) No.4, 209-214.

[16] Senthilkumar C, Ganesan G, and Karthikeyan R, "Study of electrochemical machining characteristics of Al/SiCp Composites", International Journal of Advanced Manufacturing Technology 43 (2009) 256-263.

APPENDIX

V : Voltage across tool and workpiece (V)
IEG : Inter electrode gap between tool and workpiece (mm)
EC : Electrolyte concentration (grams per litre)
FR : Flow Rate (liter per minute)
RSM : Response surface methodology
BBD : Box Behnken Design

